Journal of the Physical Society of Japan
Vol. 72, No. 12, December, 2003, pp. 3049–3052

Efficiency of Photocarrier Injection in a VO_2/TiO_2:Nb Heterostructure

Zenji HIROI*, Tohru YAMAUCHI, Yuji MURAOKA, Takaki MURAMATSU and Jun-Ichi YAMAURA

Institute for Solid State Physics, University of Tokyo, Kashiwa, Chiba 277-8581

(Received August 11, 2003)

The efficiency of photocarrier injection in a VO_2/TiO_2:Nb heterostructure is studied by measuring I–V characteristics at room temperature under ultraviolet light irradiation. It is revealed that photogenerated hole carriers in the TiO_2:Nb substrate are injected and accumulated in the VO_2 film by the photovoltaic effect. The surface charge density is controlled successfully in a wide range of 10^9–$10^{13}\,cm^{-2}$ as a function of light irradiance. The maximum hole density of $9 \times 10^{18}\,cm^{-3}$ is attained at a light irradiance of $133\,mW/cm^2$, which is estimated by assuming the uniform distribution of holes in the film. It is suggested that high efficiency can be achieved by utilizing the large dielectric constant of titanium oxide substrates.

KEYWORDS: photocarrier injection, heterostructure, transition metal oxides, VO_2, TiO_2
DOI: 10.1143/JPSJ.72.3049

Controlling the density and flow of carriers in a semiconductor is a key issue for various semiconductor devices. One of the recent trends is to induce exotic properties such as ferromagnetism through carrier control under certain external fields in a heterostructure. For example, ferromagnetic order induced by photogenerated carriers was reported in III–V semiconductor heterostructures of (In,Mn)As/GaSb.[1] Electric-field control of ferromagnetism was also reported in a field-effect transistor (FET) structure containing (In,Mn)As.[2] It is believed that these phenomena are based on the fact that ferromagnetic interactions between Mn spins are mediated by the injected hole carriers.

On the other hand, recent discoveries of many interesting phenomena in transition metal oxides (TMOs) open a possibility to use them as promising materials for electronic devices. There have been efforts in the case of oxide heterostructures to achieve carrier control using conventional semiconductor techniques: Ahn *et al.* reported successful control of hole density in a FET structure containing a copper oxide superconductor, with its critical temperature T_c varied by 5 K.[3] In a $La_{0.8}Sr_{0.2}MnO_3$ film grown on an insulating $SrTiO_3$ substrate, Katsu *et al.* observed a decrease in the Curie temperature by 10 K under ultraviolet (UV) light irradiation.[4] They suggested that electrons were injected into the film from the substrate.

Very recently, Muraoka *et al.* reported photocarrier injection in an oxide heterostructure of VO_2/TiO_2:Nb under UV light irradiation.[5] VO_2 comprising one $3d$ electron per V^{4+} ion undergoes a metal–insulator (MI) transition on cooling at a critical temperature $T_{MI} = 340$ K.[6] They fabricated a thin VO_2 film grown on a TiO_2 substrate and found that the T_{MI} is reduced to 290 K on cooling due to large epitaxial stress arising from lattice mismatch at the interface.[7] In the subsequent study, they found that the resistance of a heterostructure made of a VO_2 film and an n-type TiO_2 substrate doped with 0.05 wt% Nb decreased significantly under UV light irradiation at temperatures below T_{MI}.[5] A simple picture to explain this observation has been proposed, where only hole carriers generated by light absorption in TiO_2:Nb are injected into the VO_2 film through the interface.[5] This photocarrier injection (PCI) method has been applied to other TMOs, manganese and cupric oxides, demonstrating the generality of the method.[8,9] Particularly, in the case of a $YBa_2Cu_3O_{7-\delta}/SrTiO_3$:Nb heterostructure, the variation of T_c over 5 K was found as a result of hole doping under UV light irradiation.[10] These findings will provide us with a new strategy for the fundamental and application studies of TMOs. In this work, we study the VO_2/TiO_2:Nb heterostructure in more detail to reveal the mechanism and efficiency of PCI.

We prepared a 10-nm-thick VO_2 film epitaxially grown on the (001) surface of a Nb-doped TiO_2 single crystal substrate by pulsed laser deposition technique.[5] The nominal Nb concentration in the substrate was 0.035 wt%, which was confirmed by X-ray fluorescence analysis. This corresponds to donor concentration $N_d = 9.8 \times 10^{18}\,cm^{-3}$. Current–voltage ($I$–$V$) characteristics across the interface were measured at room temperature using a standard digital voltmeter and current source. As ohmic electrodes, gold was deposited on the VO_2 film, and copper was sputtered on the TiO_2:Nb substrate. UV light with $\lambda = 300$–400 nm from a Xe lamp was guided via a quartz opitcal fiber to illuminate the film side of the sample during the electrical measurements. The light irradiance was varied in a wide range using ND filters, and was calibrated by a light detector using the same experimental setup before the measurements. The active area of the device was assumed to be the area of the film except that of the top electrodes. The relaxation of open-circuit voltage (V_{oc}) was recorded by a digital oscilloscope under light irradiation chopped with a frequency of 10–1,000 Hz.

Figure 1 illustrates a possible band structure at 300 K expected for the VO_2/TiO_2:Nb heterostructure and the PCI process under UV light irradiation. TiO_2 is a wide-gap semiconductor with a band gap of 3.0 eV,[11] while VO_2 is a metal at 300 K above T_{MI}.[7] Thus, the band structure of the heterojunction must be essentially similar to that of a metal–semiconductor junction with a Schottky barrier. Nb^{5+} donor levels in TiO_2:Nb are located 0.1 eV below the bottom of the conduction band.[5] The Fermi level calculated from the donor density $N_d = 9.8 \times 10^{18}\,cm^{-3}$ is 0.4 eV below the bottom of the conduction band. On the other hand, the Fermi level of VO_2 may be located approximately 0.5 eV below that of TiO_2:Nb, the difference between them giving rise to a

*E-mail: hiroi@issp.u-tokyo.ac.jp

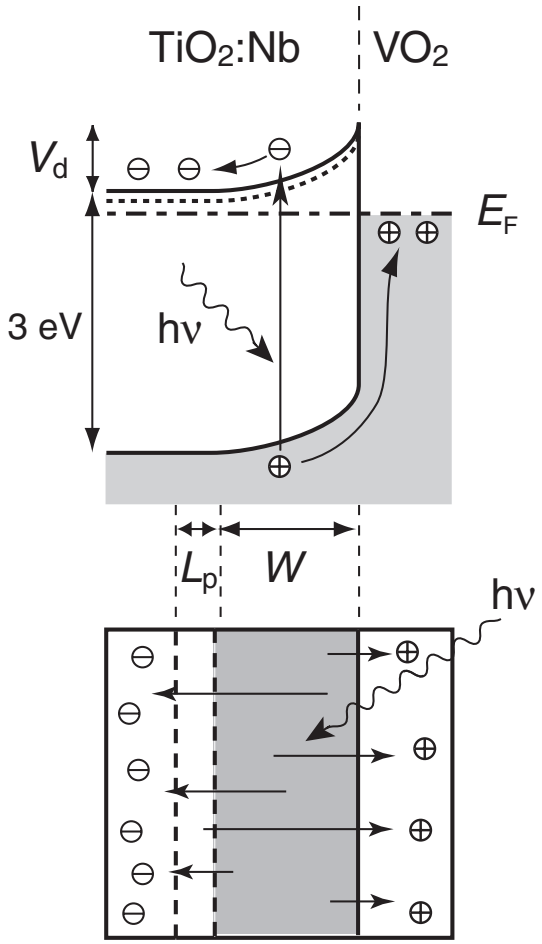

Fig. 1. Electronic band structure of a VO_2/TiO_2:Nb heterostructure at $T = 300$ K and schematic representation of the PCI process under UV light irradiation. W is the thickness of the depletion layer formed in the substrate. L_p corresponds to the diffusion length of hole carriers in TiO_2:Nb. V_d is diffusion voltage for electrons in TiO_2:Nb. Small circles with bars and crosses represent electrons and holes, respectively.

potential barrier of a height V_d and a depletion layer of a width W in the substrate. When a photon with energy larger than the band gap of TiO_2 is absorbed to create an electron–hole pair in the substrate, it is expected from this band diagram that only the hole can be injected into the film with the electron remaining in the substrate. Since the hole has much larger potential energy in TiO_2:Nb than in VO_2, this drift process must proceed quickly. In contrast, the recombination between the hole in the film and the electron in the substrate would be slow, because it should occur by tunneling across the barrier. As a result, the lifetime of the injected hole can be sufficiently long to induce substantial changes in transport properties in a steady state. Note that the hole density is adjustable with light irradiance in a wide range. Thus, we can successfully control the electronic properties of VO_2 by this PCI method. It should also be noted that essentially the same PCI is expected for a heterostructure comprising an insulating VO_2 film below T_{MI}, which is considered to be a p–n heterojunction photodiode.[5)]

In order to elucidate the PCI mechanism quantitatively and determine several parameters, we have analyzed the I–V characteristics of the VO_2/TiO_2:Nb heterostructure measured at room temperature in the dark and under UV light

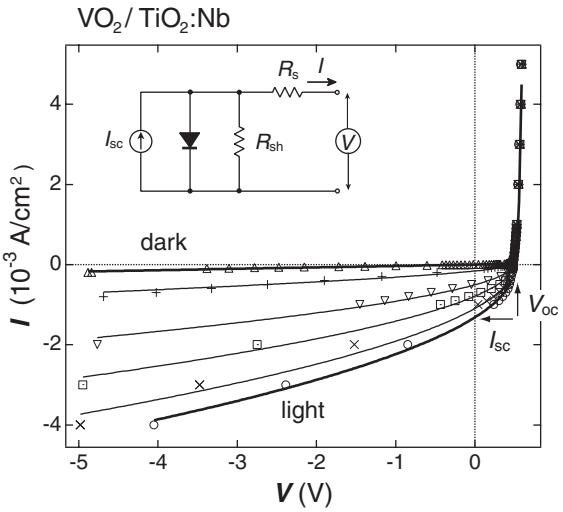

Fig. 2. I–V characteristics of a VO_2/TiO_2:Nb heterostructure measured at room temperature in the dark and under UV light irradiation. The light irradiance increases from the top to the bottom curves in the third quadrant as 0%, 10%, 25%, 50%, 75%, and 100%, where 100% refers to $L = 133\,\mathrm{mW/cm^2}$. An equivalent circuit is depicted in the figure.

illumination. As shown in Fig. 2, typical rectifying behavior is observed in the dark: the current increases rapidly around $V = 0.5$ V at a positive bias to the film, while it is small and almost independent of voltage at a negative bias with a leakage current of $0.2\,\mathrm{mA/cm^2}$ at $V = -5$ V. As the light irradiance L increases, the I–V curve shifts downward, as generally observed in a silicon photodiode, indicating additional current flow due to photogenerated carriers.[12)] I_{sc} is current density at $V = 0$ in the short-circuit condition, and V_{oc} is voltage at $I = 0$ in the open-circuit condition. The maximum light irradiance here is $133\,\mathrm{mW/cm^2}$, where $I_{sc} = 1.3\,\mathrm{mA/cm^2}$, and $V_{oc} = 0.475$ V. Thus, external quantum efficiency γ_{ex} is 3.5%, which is given by $\gamma_{ex} = (I_{sc}/e)/(L/h\nu)$, where $L/h\nu$ is the number of photons arriving and is approximately $2.3 \times 10^{17}\,\mathrm{photons/cm^2 \cdot s}$, assuming that the incident light has a wavelength of 350 nm. The γ_{ex} increases with increasing reverse bias, *e.g.*, 11% at $V = -5$ V. This value may be sufficiently large in such an unoptimized device, compared with other sophisticated UV photodetectors made of wide-gap semiconductors such as (Al,Ga)N.[13)]

A feature to be noted in Fig. 2 is the large slope in the third quadrant which increases with increasing light irradiance. In general, current in a photodiode is the sum of drift and diffusion currents, which are generated in the thin depletion layer with space charge and the neutral p and n regions, respectively.[12)] In the case of a conventional silicon photodiode, the latter is dominant because of the large mobility of carriers and small absorption of light. As a result, the photocurrent is insensitive to bias which affects only the thickness of the depletion layer. In contrast, the large slope in the I–V characteristics of Fig. 2 suggest that the drift current is much larger than the diffusion current in the present system.

We have analyzed in further detail the I–V characteristics using an equivalent circuit often used for a solarcell, as shown in the inset in Fig. 2.[12)] It contains a parallel resistance R_{sh} due to leakage current and a serial resistance R_s from the external circuit. The I–V characteristics of the

Table I. Comparison of various parameters obtained at high ($L = 133\,\mathrm{mW\,cm^{-2}}$) and low irradiance ($L = 0.01\,\mathrm{mW\,cm^{-2}}$).

L (mW cm^{-2})	$L/h\nu$ (cm^{-2}s^{-1})	V_{oc} (V)	W (nm)	Q/e (cm^{-2})	$\gamma\tau$ (s)	τ (ms)	γ (%)
133	2.4×10^{17}	0.406	12	8.8×10^{12}	3.7×10^{-5}	0.36	10
0.01	1.8×10^{13}	0.0171	30	3.2×10^{11}	1.8×10^{-2}	74	24

equivalent circuit are given by

$$I = I_0 \exp\left(-\frac{eV_d}{kT}\right)\left\{\exp\left[\frac{e(V+R_sI)}{kT}\right]-1\right\} + \frac{V+R_sI}{R_{sh}} - I_{sc}, \quad (1)$$

in the emission model for a metal-semiconductor junction which assumes that current flow is caused by thermionic emission over a barrier, neglecting all tunnel effects.[12] Ignoring the R_s in the low-current limit,

$$I = I_0 \exp\left(-\frac{eV_d}{kT}\right)\left[\exp\left(\frac{eV}{kT}\right)-1\right] + \frac{V}{R_{sh}} - I_{sc}. \quad (2)$$

The I_{sc} is given by $I_{sc} = eg_{op}(L_p + W)$, where g_{op} is the generation rate of electron–hole pairs by absorbed light (EHP/cm^3·s), L_p is the diffusion length of hole carriers, and W is the thickness of the depletion layer, as schematically depicted in Fig. 1. The W is calculated in the Schottky model to be

$$W = \left[\frac{2\varepsilon_0\varepsilon_s}{eN_d}(V_d - V)\right]^{\frac{1}{2}}, \quad (3)$$

where $\varepsilon_0 = 8.85\times10^{-14}\,\mathrm{Fcm^{-1}}$, $\varepsilon_s = 170$ for TiO_2 with an electric field parallel to the c axis,[14] and $N_d = 9.8\times10^{18}\,\mathrm{cm^{-3}}$. We have carried out the fitting of all the data sets in Fig. 2 with eq. (2). First V_d and R_{sh} are determined to be 0.486 V and 28.5 kΩ cm^2, respectively, by fitting the data obtained in the dark. Next the other data sets are well fitted with g_{op} and L_p as variable parameters. Thus, the obtained g_{op} is 2.42×10^{21} EHP/cm^3·s at $L = 133\,\mathrm{mW/cm^2}$, which decreases almost linearly with L. The L_p is small, *e.g.*, 3.5 nm at $L = 133\,\mathrm{mW/cm^2}$, and decreases slightly with decreasing L. Since the W is much larger, *e.g.*, 30 nm at $V = 0$, than L_p, most holes responsible for photocurrents are generated in the depletion layer, implying a dominant drift current. One of the reasons may be the small mobility of holes in TiO_2: they can be trapped easily as polarons.[15] Another reason is a large absorption coefficient of $\alpha \sim 10^5\,\mathrm{cm^{-1}}$ against UV light:[14] TiO_2 is known to possess a direct band gap which is almost degenerate with the indirect gap.[16] The depletion layer with $W = 30$ nm would absorb 26% of incident light, which gives the upper limit for the quantum efficiency γ_{max}. However, actual efficiency would be smaller than that, because the incident light may be reflected partly on the film surface and also absorbed in the film.

Figure 3 shows the UV light irradiation dependence of V_{oc}. A positive photovoltage to the VO_2 film increases linearly with increasing light irradiance L in a wide range of $10^{-5} < L < 10^{-1}\,\mathrm{mW/cm^2}$ and tends to saturate toward $V_d = 0.486$ V at higher irradiance. Hole doping must proceed in a rigid band at low irradiance of $V_{oc} \ll V_d$, while, at high irradiance, an effective Schottky barrier would be reduced to $V_d - V_{oc}$, resulting in the observed saturation

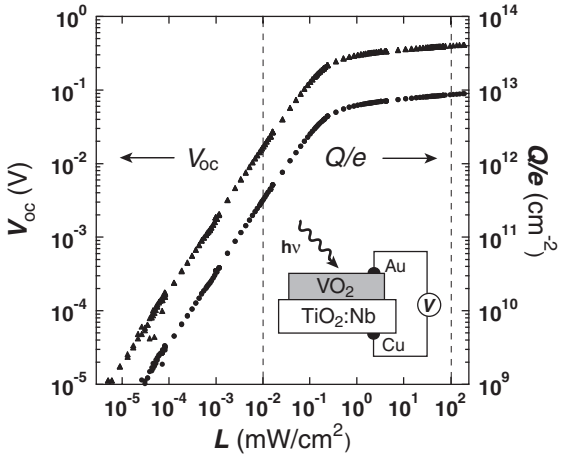

Fig. 3. Open-circuit voltage V_{oc} and surface charge density Q/e as a function of light irradiance. The data at $L = 133$ and 0.01 mW/cm^2 are listed in Table I.

of V_{oc}. By fitting the V_{oc} data to a power law L^n at low irradiance, n is found to be 0.967(2), indicating good proportionality between V_{oc} and L.

A photodiode is considered to be a condenser to accumulate photogenerated charges. Thus, we can estimate the surface density of injected holes Q/e from a simple relation of $dQ = CdV$, where C is the capacitance of the depletion layer and is given by

$$C = \frac{\varepsilon_0\varepsilon_s}{W} = \left[\frac{e\varepsilon_0\varepsilon_s N_d}{2(V_d - V_{oc})}\right]^{\frac{1}{2}}. \quad (4)$$

Carrying out the integration,

$$Q/e = \left(\frac{2\varepsilon_0\varepsilon_s N_d}{e}\right)^{\frac{1}{2}}\left[V_d^{\frac{1}{2}} - (V_d - V_{oc})^{\frac{1}{2}}\right]. \quad (5)$$

The obtained Q/e is plotted in Fig. 3. In the case of $V_{oc} \ll V_d$, the C is constant and thus $Q = CV$.

On the other hand, the efficiency of carrier accumulation should depend on the generation and recombination process of photoexcited carriers. Assuming that a photon is transferred to a hole with internal quantum efficiency γ and also that an injected hole has a lifetime τ, accumulated charge density is given by

$$Q/e = \gamma\frac{L}{h\nu}\tau. \quad (6)$$

At low irradiance with $V_{oc} \ll V_d$, both γ and τ must be independent of L, and thus Q is proportional to L. Therefore, we expect a linear relation between V_{oc} and L, as observed in Fig. 3. At high irradiance, however, γ must decrease with increasing L, because the thickness of the depletion layer decreases as in eq. (3) with increasing V_{oc}. Moreover, τ must also decrease rapidly with increasing L, because the effective height of the Schottky barrier is reduced. As a result, Q is

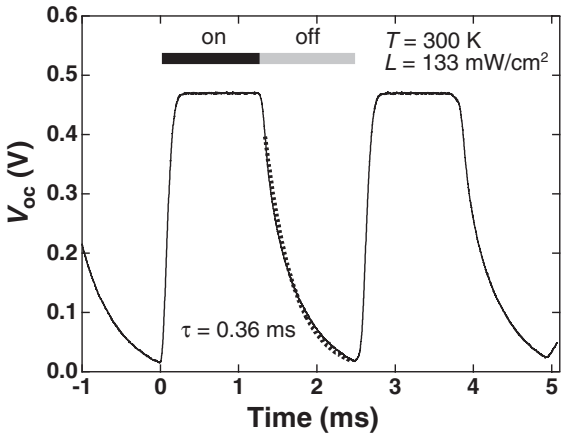

Fig. 4. Relaxation of V_{oc} measured at $T = 300\,\mathrm{K}$ and $L = 133\,\mathrm{mW/cm^2}$. The dotted curve is a fit to a single exponential form, $\exp(-t/\tau)$, with $\tau = 0.36\,\mathrm{ms}$.

suppressed at high irradiance as observed in Fig. 3.

To exemplify this, let us compare the two typical cases with $L = 133$ and $0.01\,\mathrm{mW/cm^2}$. From eqs. (5) and (6), Q/e and $\gamma\tau$ are obtained as listed in Table I. In order to estimate the lifetime, the relaxation of V_{oc} has been measured using an oscilloscope at $L = 133\,\mathrm{mW/cm^2}$, as shown in Fig. 4. The V_{oc} decreases almost exponentially after the light was turned off. By fitting the decay curve to a single exponential form, we obtain $\tau = 0.36\,\mathrm{ms}$, which gives the quantum efficiency of 10%. However, this is just a rough estimation, because τ must change with V_{oc}. On one hand, the maximum value γ_{max} that is expected from light absorption only in the depletion layer is 11% with $W = 12\,\mathrm{nm}$. This coincidence suggests that the above estimation is reasonable. We tried to determine γ at $L = 0.01\,\mathrm{mW/cm^2}$ in the same experimental setup, but could not because τ was too long for measurement. Thus, we measured the decrease of V_{oc} using a voltmeter immediately after the light had been switched off and obtained $\tau = 74\,\mathrm{ms}$, which is 200 times larger than that at high irradiance. Apparently, this long lifetime is caused by the large Schottky barrier for electrons at the junction. Then, γ at low irradiance is calculated to be 24%, which is again very close to $\gamma_{max} = 26\%$ expected for $W = 30\,\mathrm{nm}$. It is important to note that the efficiency of PCI is governed by the light absorption process at low irradiance, while is determined by the capacitance at high irradiance.

Finally, we will briefly discuss the maximum density of holes to be injected into the film. That obtained for the present system is $Q/e = 8.8 \times 10^{12}\,\mathrm{cm^{-2}}$. Assuming the uniform distribution of holes in the 10-nm-thick VO_2 film, the hole density Δp is $8.8 \times 10^{18}\,\mathrm{cm^{-3}}$, which corresponds to only 0.0004 hole per V atom. This is apparently too small to expect a substantial change in the physical properties for TMOs. It is plausible, however, that the actual hole density near the interface is larger than that, because of the internal electrostatic potential at the junction.

A challenge in the future will be to determine how to achieve larger efficiency. It would be critical to increase the dielectric constant of the substrate. In fact, the major reason that PCI has worked successfully in oxide heterostructures is found in the large ε_s of TiO_2 (170) or $SrTiO_3$ (330) at room temperature, compared with those of conventional semiconductors ($\sim$10). Further enhancement in ε_s would result in higher efficiency. In this sense, $SrTiO_3$ is a promising material as a substrate, because it exhibits exceptionally large ε_s up to 20,000 at temperatures below 100 K due to quantum paraelectricity.[17] We have actually observed a change in hole density of a few percent in a $YBa_2Cu_3O_{7-\delta}$ film grown on a $SrTiO_3$:Nb substrate at $T \sim 40\,\mathrm{K}$.[10] Further experiments are under way on various TMOs at low temperatures.

Acknowledgments

We thank Hisashi Homma of Rigaku for assistance in X-ray fluorescence analysis. This research was supported by a Grant-in-Aid for Scientific Research on Priority Areas (A) and a Grant-in-Aid for Creative Scientific Research given by the Ministry of Education, Culture, Sports, Science and Technology.

1) S. Koshihara, A. Oiwa, M. Hirasawa, S. Katsumoto, Y. Iye, C. Urano, H. Takagi and H. Munekata: Phys. Rev. Lett. **78** (1997) 4617.
2) H. Ohno, D. Chiba, F. Matsukura, T. Omiya, E. Abe, T. Dietl, Y. Ohno and K. Ohtani: Nature **408** (2000) 944.
3) C. H. Ahn, J.-M. Triscone, N. Archibald, M. Decroux, R. H. Hammond, T. H. Geballe, O. Fischer and M. R. Beasley: Science **269** (1995) 373.
4) H. Katsu, H. Tanaka and T. Kawai: Appl. Phys. Lett. **76** (2000) 3245.
5) Y. Muraoka, T. Yamauchi, Y. Ueda and Z. Hiroi: J. Phys.: Condens. Matter **14** (2002) L757.
6) F. J. Morin: Phys. Rev. Lett. **3** (1959) 34.
7) Y. Muraoka and Z. Hiroi: Appl. Phys. Lett. **80** (2002) 583.
8) Y. Muraoka and Z. Hiroi: J. Phys. Soc. Jpn. **72** (2003) 781.
9) T. Muramatsu, Y. Muraoka, T. Yamauchi, J. Yamaura and Z. Hiroi: to be published in J. Magn. Magn. Mater.
10) Y. Muraoka, T. Yamauchi, T. Muramatsu, J. Yamaura and Z. Hiroi: to be published in J. Magn. Magn. Mater.
11) Z. M. Jarzebski: *Oxide semiconductors* (Pergamon Press, Oxford, 1973).
12) A. G. Milnes and D. L. Feucht: *Heterojunctions and metal–semiconductor junctions* (Academic Press, New York, 1972).
13) C. J. Collins, U. Chowdhury, M. M. Wong, B. Yang, A. L. Beck, R. D. Dupuis and J. C. Campbell: Appl. Phys. Lett. **80** (2002) 3754.
14) M. W. Ribarsky: *Handbook of optical constants of solids*, ed. E. D. Palik (Academic Press, Orlando, 1985), p. 795.
15) A. J. Bosman and H. J. Van Daal: Adv. Phys. **19** (1970) 1.
16) B. Poumellect, P. J. Durham and G. Y. Guo: J. Phys.: Condens. Matter **3** (1991) 8195.
17) K. A. Muller and H. Burkard: Phys. Rev. B **19** (1979) 3593.